CARBOXYLATED CELLULOSE NANOFIBERS AS A NOVEL EFFICIENT ADSORBENT FOR WATER PURIFICATION

RAGAB E. ABOU-ZEID,[*] AHMED SALAMA,[*] ZEHBAH ALI AL-AHMED,[**]
NASSER S. AWWAD[***] and MAHA A. YOUSSEF[****]

[*]*Cellulose and Paper Department, National Research Centre, 33 El-Bohouth Str.,
Dokki, P.O. 12622, Giza, Egypt*
[**] *College of Art and Sciences - Dhahran Aljounb,
King Khalid University, Saudi Arabia*
[***] *Department of Chemistry, Faculty of Science,King Khalid University, P.O. Box 9004, Abha 61413, Saudi
Arabia*
[****]*Analytical Chemistry and Control Department, Hot Laboratories Center, Atomic Energy Authority of
Egypt, P.O. 13759 Abu Zaabal, Cairo, Egypt*
✉ *Corresponding author: R. E. Abou-Zeid, r_abouzeid2002@yahoo.com*

Cellulose nanofibers (CNF) containing carboxylic groups were prepared through sequence oxidation steps. TEMPO-periodate-chlorite oxidation steps of bleached cellulose pulp, extracted from bagasse, were carried out. The carboxyl content measurements revealed that, mostly, cellulose nanofibers with tricarboxylic groups for each anhydroglucose unit were formed (3.5 mmol g^{-1}). The highly carboxylated CNF (TPC-CNF) were studied by FTIR, AFM, SEM and TEM techniques. TPC-CNFs were examined to eliminate methylene blue (MB) from synthetic solutions and compared with TEMPO-oxidized CNF (T-CNF). The best interpretation of the adsorption results was given by the pseudo-first order and Langmuir isotherm models, with maximum adsorption capacity of 502 mg/g, compared to conventional T-CNF, which reached 409 mg/g. TPC-CNF displayed high adsorption capacity in a slightly basic medium. This article presents a novel biodegradable and sustainable adsorbent for organic dye removal.

Keywords: cellulose, TEMPO oxidized cellulose nanofiber, MB removal, water purification

INTRODUCTION

Organic dyes result as wastes from several industries, such as textiles, ceramics, and leather tanning. Organic dyes are complex molecules, not biodegradable and their discharge into water affects the photosynthetic activity in aquatic life.[1–3] The adsorption technique has emerged as an economical, efficient and sustainable strategy for the detoxification of organic pollutants and metal ions.[4,5] In the last decades, cellulose, which is the most abundant polymer on the earth, has been used as a sustainable and biodegradable adsorbent for various pollutants.[6–9] However, the absence of active functional groups hinders its application as an efficient adsorbent. Many trials have been conducted to improve the adsorption capacity of cellulose. For example, a cellulose-lysine Schiff-base-based sensor was utilized as adsorbent for Hg(II) detoxification of aqueous solutions.[10] Salama prepared cellulose/soy protein isolate/hydroxyapatite as a sustainable bioactive material for adsorption of MB from aqueous solutions.[11]

Cellulose nanofibers (CNF) are a very attractive topic owing to their fascinating properties, such as high strength, low density and high viscosity.[12,13] CNF have been applied as high value-added materials resulting from sustainable materials.[14] There are many literature reports on the usage of CNF as reinforcement for paper, in coatings,[15] nanopapers,[16] and recent biomedical applications.[17] CNF can be prepared by applying suitable mechanical shearing that supports the release of microfibrils, with less than 100 nm in width and a few micrometers in length.[6] There are many pretreatments that can be used to produce CNF, such as enzymatic and chemical pretreatments. Among them, 2,2,6,6-tetramethylpiperidine-1-oxyl (TEMPO) oxidation

has become a widely used method. TEMPO-mediated oxidization reaction can produce a carboxylic group with selective oxidation of C6 of the anhydrogluciose unit, which promotes the adsorption capacity of cationic species on its surface.[18,19] The previously mentioned technique is currently utilized as a pretreatment to produce carboxylated groups on the surface of CNF for different types of applications. Consequently, the produced CNF are presented as a sustainable alternative with distinctive potential for the elimination of cationic and anionic dyes from wastewater.

Among recent trials, the elimination of toxic metals, such as Cu^{2+}, radioactive metal ions (UO_2^{2+}), Ni^{2+} and Cr^{3+6}, using CNF was reported. Sehaqui *et al.* studied the adsorption capacity of Cu^{2+} onto unmodified CNF and TEMPO-oxidized CNF, and found adsorption values of 13 and 112 mg/g, respectively. It can be noticed that after TEMPO oxidation, the adsorption capacity increased by more than eight times.[20] Srivastava *et al.* reported the effect of the degree of oxidation on the adsorption capacity of Cd^{2+}, Pb^{2+}, Ni^{2+} and Cr^{3+} from wastewater, and a 3-10% higher effectiveness compared to that of unmodified CNF.[21] The removal efficiency of cellulose nanofibers towards a broad range of contaminants was enhanced by phosphorylation. Bacterial cellulose was phosphorylated, stabilizing its microfibrous structure, and used as adsorbent for different metal ions, such as Cu^{2+}, Mn^{2+}, Zn^{2+}, Co^{2+}, Fe^{3+}, and lanthanide ions, such as La^{3+}, Sm^{3+}, Ho^{3+}.[22] Cellulose nanocrystals (CNC) and cellulose nanofibers were phosphorylated and showed higher adsorption capacity towards Ag+, Cu^{2+}, and Fe^{3+}, compared to unmodified nanomaterials.[23] Moreover, CNF prepared from kenaf were applied as adsorbent for cationic methylene blue.[24] Mohamed *et al.* prepared cellulose nanocrystals alginate beads as a sustainable material for MB adsorption. The hydrogel beads showed maximum adsorption capacity of 265.4 mg/g and the removal efficiency reached 97% after five adsorption-desorption cycles. Cellulose/graphene oxide fiber was developed by the wet spinning technique and used as adsorbent for MB dye. The maximum adsorption reached 480.8 mg/g, according to the Langmuir model, and the fibers could be recycled three times.[25] Surface quaternized cellulose nanofibers were prepared by treating mechanically disintegrated wood pulp with glycidyltrimethylammonium chloride. These fibers showed high tensile strength, high porosity, high water absorbency and capability for anionic dyes adsorption.[26,27]

In order to increase the carboxyl content of cellulose nanofibers, another method of oxidation applied was the periodate oxidation of CNF, to produce 2, 3-dialdehyde groups along cellulose units, which was followed by chlorite oxidation of these aldehyde groups to carboxylic groups. This method allowed increasing the carboxyl content of the cellulose nanofibers, compared to TEMPO-oxidized CNF. The high density of carboxyl groups on CNF will increase the adsorption of cationic species from aqueous solutions.

In this study, the combination of TEMPO oxidation of cellulose nanofiber with the periodate/chlorite method was studied to produced high negatively charged tricarboxylic CNFs. The adsorption capacity of TEMPO-oxidized CNFs and tricarboxylic CNFs towards MB from wastewater were investigated. The factors controlling the removal efficiency, such as solution pH, soaking time and dye concentration, were examined.

EXPERIMENTAL

Materials

The raw material used in this study was bleached bagasse pulp supplied from Qena Company of Paper Industry, Egypt, with the following chemical composition: α-cellulose 71%, hemicelluloses 27% and ash 0.9%. 2,2,6,6-Tetramethylpiperidine-1-oxyl (TEMPO), sodium metaperiodite ($NaIO_4$), sodium bromide (NaBr) and methylene blue (MB) were purchased from Sigma Aldrich. All chemicals were used without further purification.

TEMPO-periodate-chlorite oxidation processes

TEMPO oxidized bagasse pulp was prepared as previously described.[28–30] Shortly afterwards, 20 g of bleached bagasse pulp was dispersed in distilled water with TEMPO (0.8 g) and sodium bromide (8 g). Then, 300 mL of sodium hypochlorite solution (15%) was added under continuous stirring and the pH was adjusted to 10 using NaOH solution (3M). At the end of the reaction, the pH was adjusted to 7 and the product was centrifuged at 10000 rpm several times. Finally, the product was purified by dialysis for 1 week against deionized water. T-CNF was prepared using a Masuko grinder for mechanical defibrillation treatment.

TEMPO oxidized cellulose nanofibers (T-CNF) were oxidized by periodate-chlorite oxidation to acquire more carboxylate groups, according to a procedure described previously by Abou-Zeid et al.[31] In brief, 10 g of TEMPO cellulose nanofibers diluted

to 1% were heated to 60 °C in a water bath. Then, 46 mmol of sodium metaperiodite (NaIO₄) was added and the reaction was stopped after 3 hours. In the second step, 4.5 g of dialdehyde CNF was diluted to a certain consistency and 50 mmol of sodium chlorite (NaClO₂) was added, followed by adding 60 mL of 20% acetic acid. The resulting tricarboxylate CNF (TPC-CNF) was washed and filtered.

Determination of carboxylate content

The electric conductivity titration method was used to determine the total carboxylate content of T-CNF and TPC-CNF.[31,32] In brief, a dried sample (~50 mg) was carefully mixed with 0.01 M HCl (15 mL) and deionized water, and was titrated with standard NaOH. The carboxylate content, C (mmol/g), was calculated using Equation (1):

$$C = ((V_1 - V_o) \times C_{NaOH}) / m \qquad (1)$$

where V_1 and V_o are the volumes of NaOH before and after titration, C_{NaOH} is the concentration of NaOH, and m is the weight of the dried sample.

Characterization

Fourier transform infrared spectroscopy (FT-IR) of cellulose pulp, T-CNF and TPC-CNF was carried out on Mattson 5000 equipment. Scanning electron microscopy (SEM) was performed on a Quanta 250 Model FEG (Field Emission Gun). Transmission electron microscopy (TEM) images were collected with a JEOL JEM-2100 electron microscope at 100k× magnification. The prepared T-CNF and TPC-CNF were characterized by AFM, using AFM Multimode (DI, Veeco, Instrumentation Group) in the trapping mode, with multi 130 tips. X-ray diffraction patterns (XRD) were recorded using an X-ray diffractometer (PANalytical, Netherlands) at room temperature, with a monochromatic Cu K radiation source (λ (wavelength) = 1.5418 A), with a 2Ө angle ranging from 4° to 60°. The crystallinity index was calculated using Segal's method:[33]

$$\text{Crystalinity \%} = 1 - (I_{am}/I_{002}) \times 100 \qquad (2)$$

where I_{200} represents the crystalline material and I_{am} represents the amorphous one.

Adsorption study

The adsorption capacity of the developed materials was evaluated using the batch method technique. For adsorption experiments, 0.1 g of freeze-dried TPC-CNF was soaked in 50 mL dye solution. After the adsorption process was complete under the desired conditions, the solution was immediately separated from the adsorbents and the dye concentration was measured at 630 nm to calculate the adsorption capacity.

Scheme of TPC-CNF preparation and absorption process

In the current study, cellulose pulp was extracted from sugarcane bagasse, which was cultivated in Upper Egypt (Qena Company for paper making), according to our previous work.[31,34] It was reported that the stable nitroxyl radical TEMPO can be used as selective oxidizing agent for the primary hydroxyl group oxidation, along with the mechanical defibrillation process.[35] The formed T-CNF was subjected to a further oxidation step in order to increase the carboxylic content. The second oxidation step was the selective oxidation of the hydroxyl groups in C_2 and C_3 using periodate/chlorite oxidation. This oxidation step generated TPC-CNF, as shown in Scheme 1.
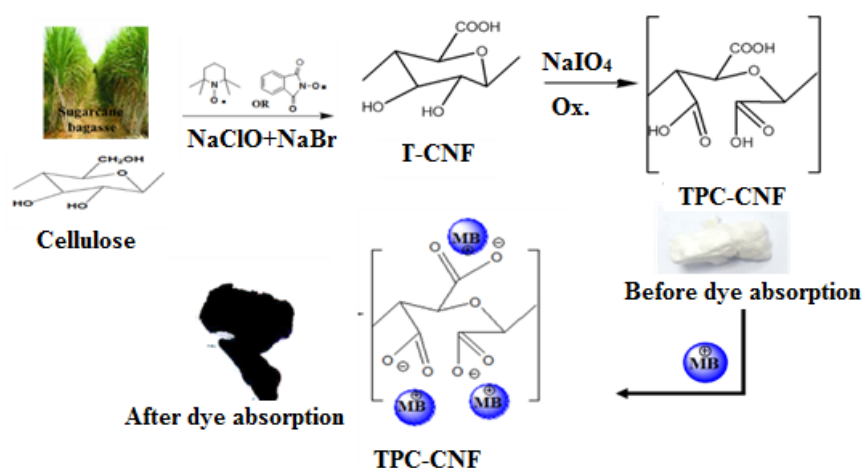
Scheme 1: Scheme of prepared TPC-CNF and the absorption process

RESULTS AND DISCUSSION

In order to increase the carboxyl content of cellulose nanofibers, further oxidation was applied to T-CNF by the periodate oxidation method to produce 2, 3 dialdehyde groups, along the cellulose units, which was followed by

chlorite oxidation of these aldehyde groups to carboxylic acid groups. This method allows increasing the carboxyl content of cellulose nanofibers, compared to the initial T-CNF. The high density of the carboxyl groups on CNF will increase the adsorption capacity towards cationic species in aqueous solutions.

Carboxylated cellulose nanofibers

The carboxylate content of CNF was calculated after TEMPO and periodate/chlorite oxidation. The results showed that T-CNF and periodate/chlorite CNF contained 0.9 and 3.5 mmol/g, respectively. This result confirms that the anhydroglucose unit of CNF, further oxidized with the periodate/chlorite system, mostly contains three carboxylate groups, and was denoted as TPC-CNF.

Figure 1 shows the FT-IR spectra of cellulose, T-CNF and TPC-CNF. The spectra reveal the characteristic peaks for cellulose. The band located at 3440 cm^{-1} is assigned to the stretching vibration of –OH groups, that at 2928 cm^{-1} corresponds to the stretching vibration of C-H and CH$_2$ groups, and that at 1015 cm^{-1} is due to the CH$_2$-O-CH$_2$ stretching vibration. A new band appeared at 1744 cm^{-1} after oxidation, which is assigned to C=O stretching vibration. The intensity of this peak increased after further oxidation with periodate/chlorite, as seen in Figure 1.

X-ray diffraction

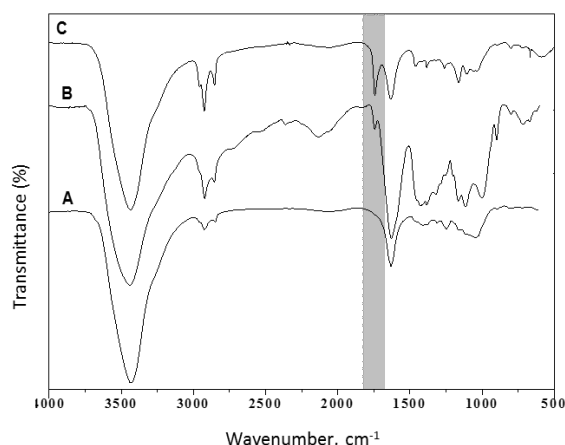XRD diffractograms of cellulose, T-CNF and TPC-CNF are presented in Figure 2. The major

diffraction peaks at 2-Theta of 15, 18 and 23°, which are indexed as (101), (10ī) and (002), were observed. These signals are characteristic of cellulose I. The crystallinity percent of all the samples were calculated from the ratio of the height of the (002) peak (I$_{002}$) and the height of the minimum (I$_{AM}$) between the 002 and the 101 peaks. This method was developed by Segal and coworkers,[33,36] and using it, we obtained values of 55, 83 and 59% for cellulose, T-CNF and TPC-CNF, respectively. It can be noticed that the crystallinity increased after TEMPO oxidation as a result of the degradation of the amorphous parts caused by oxidation. However, this value decreased again with further oxidation using the periodate/chlorite method, which suggests the CNF underwent a certain degree of degradation.

Morphology of oxidized cellulose nanofibers

The TEM and AFM images of dispersed T-CNF and TPC-CNF are shown in Figure 3. After TEMPO-oxidation treatment, the diameter of the fibers is around 20 nm, with different lengths – up to a few micrometers. After periodiate/chlorite oxidation, the fibers become smaller in diameter and length, due to the degradation of these fibers through this additional oxidation process. Also, the increase in the carboxylic content from 0.9 to 3.5 is expected to increase the repulsion forces among the fibers. TEM and AFM results also reveal that the TPC-CNF are finer in shape, compared to T-CNF, which means that the aspect ratio increased, as illustrated in Figure 3 (B and D).

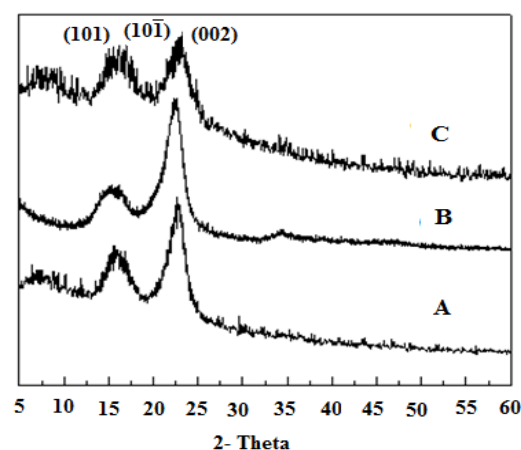Figure 1: FT-IR spectra of (A) cellulose pulp, (B) T-CNF and (C) TPC-CNF

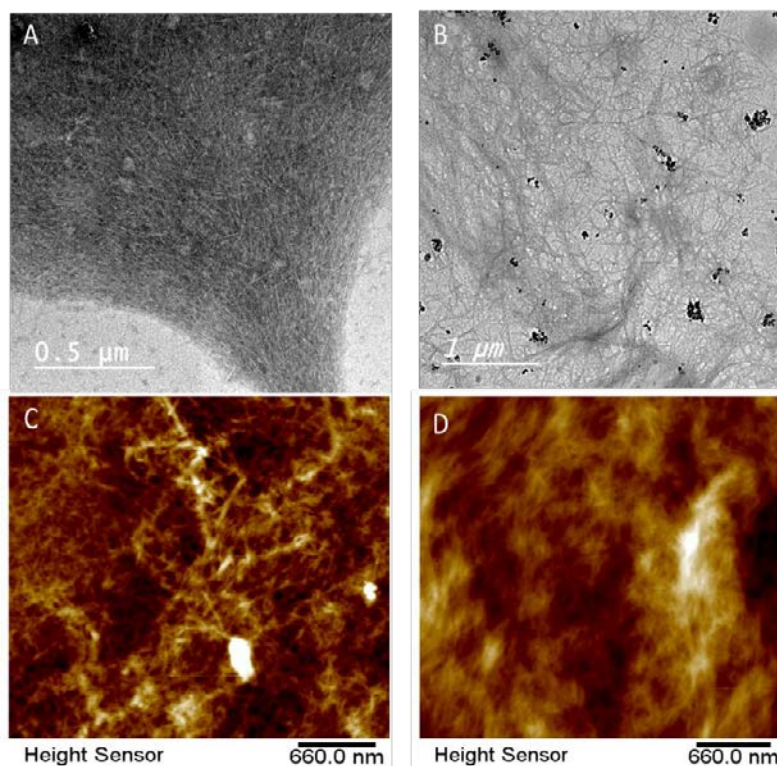Figure 2: XRD diffractograms of (A) cellulose, (B) T-CNF and (C) TPC-CNF

Figure 3: TEM (up) and AFM (down) of T-CNF (A and C) and TPC-CNF (B and D), respectively
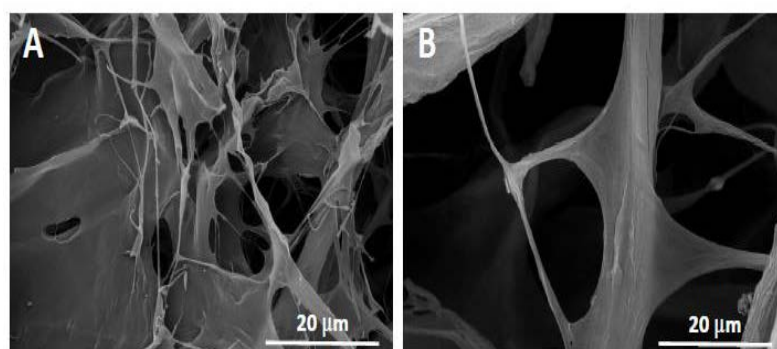

Figure 4: SEM of T-CNF (A) and TPC-CNF (B)

Figure 4 shows the morphology of T-CNF and TPC-CNF observed by SEM. The images illustrate that the further oxidation of T-CNF to tricarboxylic CNF does not significantly change the morphology of the nanofibers, the only difference from T-CNF seems to be a slight decrease in the fiber diameters. Moreover, the fibers become finer in shape, which further confirms the degradation of CNF fibers upon further oxidation.

Adsorption study

The adsorption properties of T-CNF and TPC-CNF were assessed in the current study. The pH of any solution influences the ionization level of the ions, promoting the ionic property of the adsorbent.[37] The effect of pH on the adsorption capacity of T-CNF and TPC-CNF was evaluated and the results are shown in Figure 5. The results showed that the adsorption of MB gradually increased to reach the optimum value at pH 6. The adsorption capacity recorded 75 and 94 mg/g for T-CNF and TPC-CNF, respectively. TPC-CNF exhibited a higher adsorption capacity, compared with T-CNF. This performance proved the role of the carboxylate anion content in the two materials, which provides effective sites for electrostatic interaction with cationic MB molecules. These

results demonstrate that the density of the carboxylate anion is an important factor that controls the adsorption capacity of the oxidized cellulose.

The rate of MB uptake depends on the contact time between the oxidized cellulose and the dye solution.[38] The adsorption of MB onto T-CNF and TPC-CNF presents a rapidly increasing trend through the first 30 minutes, with no further considerable increase achieved after this time. Equilibrium was achieved after 40 minutes, as displayed in Figure 6.

The pseudo-first and –second order models are shown in Equations (3) and (4), respectively:

$$\log (q_e - q_t) = \log (q_e) - \frac{K1}{2.303} t \qquad (3)$$

$$\frac{t}{qt} = \frac{t}{qe} + \frac{1}{k2qe2} \qquad (4)$$

The parameters of the kinetic models for T-CNF and TPC-CNF were calculated and displayed in Table 1. The calculated correlation coefficients (R^2) for the oxidized cellulose indicated that the adsorption of MB onto T-CNF and TPC-CNF followed the pseudo-second order model. These results suggest that the chemical

bonds between MB and oxidized cellulose nanofibers controlled the adsorption.

Figure 7 proves the effect of MB content on its adsorption onto T-CNF and TPC-CNF. MB elimination increases to 340 and 441 mg/g for T-CNF and TPC-CNF, respectively, at the MB content of 500 ppm. The adsorption capacity tends to level off when higher concentrations of MB were used.

The Langmuir isotherm parameters were calculated based on Equation 5:[39]

$$\frac{C_e}{q_e} = \frac{K_s}{q_{max}} + \frac{C_e}{q_{max}} \qquad (5)$$

The correlation coefficient of MB adsorption was calculated and presented in Table 2. The high values of the correlation coefficients ($R^2 > 0.97$ and 0.98 for T-CNF and TPC-CNF, respectively) illustrate that the Langmuir equation describes better the adsorption of MB onto T-CNF and TPC-CNF. The parameter q_{max} recorded the following values: 413 and 500 mg/g for T-CNF and TPC-CNF, respectively.
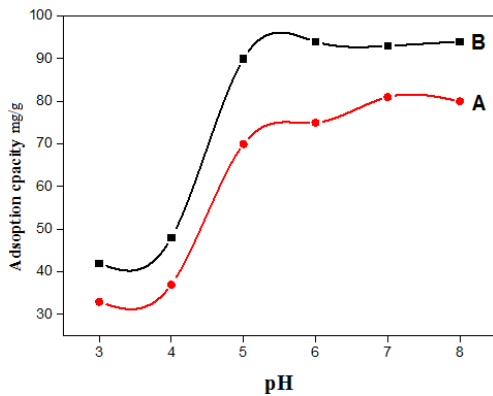

Figure 5: Effect of pH on the adsorption capacity of T-CNF (A) and TPC-CNF (B) towards MB (MB concentration: 100 mg/L; oxidized cellulose: 0.05 g/50 mL and contact time: 60 min)
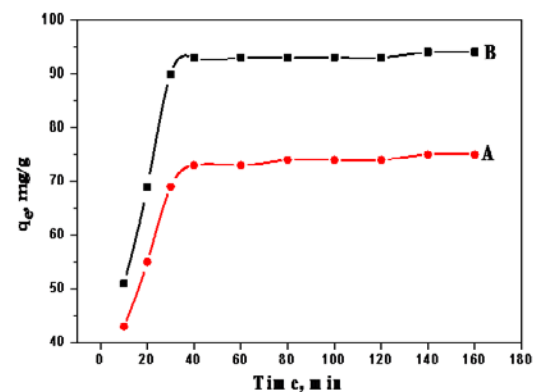

Figure 6: Effect of time on the adsorption capacity of T-CNF (A) and TPC-CNF (B) towards MB (MB concentration: 100 mg/L; oxidized celulose: 0.05 g/50 mL and pH 6)

Table 1
Kinetic parameters calculated for T-CNF and TPC-CNF

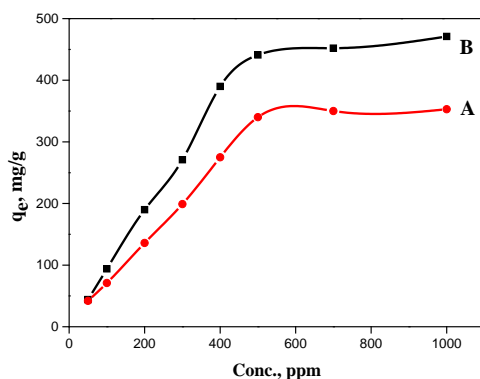| Sample	Pseudo-first order model				Pseudo-second order model		
	$q_{e \cdot exp}$ (mg/g)	$q_{e \cdot cal}$ (mg/g)	K_1 (min^{-1})	R^2	$q_{e \cdot cal}$ (mg/g)	K_2 (g(mg min)$^{-1}$)	R^2
T-CNF	75	35	0.0046	0.46	78.3	22.4 x 10^{-4}	0.998
TPC-CNF	94	22	0.036	0.54	99	17.2 x 10^{-4}	0.995

Figure 7: Effect of MB content on the adsorption capacity of T-CNF (A) and TPC-CNF (B),
(oxidized cellulose: 0.05 g/50 mL, pH 7 and adsorption time 24 hours)

Table 2
Parameters for MB adsorption onto T-CNF and TPC-CNF

Sample	Langmuir isotherm constants			Freundlich isotherm constants		
	K_s (mg/L)	q_m (mg/g)	R^2	P (mg/g)	N	R^2
T-CNF	92.19	409	0.97	14.3	1.82	0.87
TPC-CNF	23.2	502	0.989	64	2.71	0.5

Table 3
Maximum MB adsorption onto various cellulose derived materials

Adsorbent	Maximum adsorption of MB (mg/g)	References
Cellulose grafted SPI/hydroxyapatite hybrid	454	11
Carboxymethyl cellulose-g-polymethacrylic acid/calcium phosphate	180.2	7
Cellulose nanocrystal/alginate	256.4	25
Cellulose/graphene oxide fibers	480.8	40
TEMPO oxidized CNC	217.4	41
TPC-CNF	502	This work

The Freundlich model is presented in Equation 6:

$$\log q_e = \frac{1}{n}\log C_e + \log P$$

(6)

Low values of the linear coefficient for the Freundlich model (0.87 and 0.5 for T-CNF and TPC-CNF, respectively) were calculated. Moreover, the values of *P* and *n* constants were 14.3 and 1.82 for T-CNF, and 45 and 2.3 for TPC-CNF, respectively. These results proved that this model is not appropriate for describing the adsorption of MB onto TPC-CNF.

A comparison of TPC-CNF with other adsorbents investigated for MB adsorption is presented in Table 3. TPC-CNF nanofibers exhibited high MB adsorption values, compared with those for other cellulosic materials reported in previous studies.

CONCLUSION

A novel cellulose derivative, TPC-CNF, was prepared from bleached bagasse pulp after TEMPO-periodate-hypochlorite oxidation steps. The carboxyl content revealed that the anhydroglucose unit in the oxidized cellulose nanofibers mostly contained three carboxylic groups. TEM and AFM observations revealed that the oxidized fibers were around 20 nm wide and a few micrometers long. The adsorption capacity of TPC-CNF for MB was favorable in a slightly alkaline medium. MB adsorption onto TPC-CNF was described well by the pseudo-second order and Langmuir isotherm models, as the materials exhibited an adsorption capacity of 499 mg/g. This work introduces an alternative biocompatible adsorbent, TPC-CNF, with high adsorption ability towards organic pollutants.

REFERENCES

[1] R. Fabryanty, C. Valencia, F. E. Soetaredjo, J. N. Putro, S. P. Santoso *et al.*, *J. Environ. Chem. Eng.*, **5**, 5677 (2017), https://doi.org/10.1016/j.jece.2017.10.057

[2] A. Salama and P. Hesemann, *J. Polym. Environ.*, **26**, 1986 (2018), https://doi.org/10.1007/s10924-017-1093-3

[3] A. Salama, S. Etri, S. A. A. Mohamed and M. El-Sakhawy, *Carbohyd. Polym.*, **189**, 138 (2018), https://doi.org/10.1016/j.carbpol.2018.02.016

[4] K. Varaprasad, T. Jayaramudu and E. Rotimi, *Carbohyd. Polym.*, **164**, 186 (2017), https://doi.org/10.1016/j.carbpol.2017.01.094

[5] M. Monier, D. M. Ayad, Y. Wei and A. A. Sarhan, *J. Hazard. Mater.*, **177**, 962 (2010), https://doi.org/10.1016/j.jhazmat.2010.01.012

[6] R. E. Abou-Zeid, R. Khiari, N. El-Wakil and A. Dufresne, *Biomacromolecules*, **2**, 573 (2018), https://doi.org/10.1021/acs.biomac.8b00839

[7] A. Salama, *Environ. Nanotechnol. Monit. Manag.*, **6**, 159 (2016), https://doi.org/10.1016/j.enmm.2016.10.003

[8] A. Salama, *Int. J. Biol. Macromol.*, **106**, 940 (2018), https://doi.org/10.1016/j.ijbiomac.2017.08.097

[9] A. Salama, M. A. Diab, R. E. Abou-Zeid, H. A. Aljohani and K. R. Shoueir, *Compos. Commun.*, **7**, 7 (2018), https://doi.org/10.1016/j.coco.2017.11.006

[10] S. Kumari and G. S. Chauhan, *ACS Appl. Mater. Interfaces*, **6**, 5908 (2014), https://doi.org/10.1021/am500820n

[11] A. Salama, *J. Colloid. Interface Sci.*, **487**, 348 (2017), https://doi.org/10.1016/j.jcis.2016.10.034

[12] M. El Bakkari, V. Bindiganavile, J. Goncalves and Y. Boluk, *Carbohyd. Polym.*, **203**, 238 (2019), https://doi.org/10.1016/j.carbpol.2018.09.036

[13] A. Salama, *Int. J. Biol. Macromol.*, **127**, 606 (2019), https://doi.org/10.1016/j.ijbiomac.2019.01.130

[14] A. Salama, R. E. Abou-Zeid, I. Cruz-Maya and V. Guarino, *Carbohyd. Polym.*, **229**, 115472 (2020), https://doi.org/10.1016/j.carbpol.2019.115472

[15] M. Delgado-Aguilar, *Cellulose*, **25**, 683 (2018), https://doi.org/10.1007/s10570-017-1572-7

[16] Q. Tarrés, S. Boufi, P. Mutjé and M. Delgado-Aguilar, *Cellulose*, **24**, 3943 (2017), https://doi.org/10.1007/s10570-017-1394-7

[17] R. E. Abouzeid, R. Khiari, D. Beneventi and A. Dufresne, *Biomacromolecules*, **11**, 4442 (2018), https://doi.org/10.1021/acs.biomac.8b01325

[18] M. Hassan, R. Abou-Zeid, E. Hassan, L. Berglund, Y. Aitomäki *et al.*, *Polymers*, **8**, 1 (2017), https://doi.org/10.3390/polym9080335

[19] G. Biliuta, D. Suteu, T. Malutan, A. I. Chirculescu, I. Nica *et al.*, *Cellulose Chem. Technol.*, **52**, 609 (2018), http://www.cellulosechemtechnol.ro/pdf/CCT7-8(2018)/p.609-618.pdf

[20] H. Sehaqui and U. Perez, *Cellulose*, **21**, 2831 (2014), https://doi.org/10.1007/s10570-014-0310-7

[21] S. Srivastava, A. Kardam and K. R. Raj, *Int. J. Green Nanotechnol. Biomed.*, **4**, 46 (2012), https://doi.org/10.1080/19430892.2012.654744

[22] T. Oshima, K. Kondo, K. Ohto, K. Inoue and Y. Baba, *React. Funct. Polym.*, **68**, 376 (2008), https://doi.org/10.1016/j.reactfunctpolym.2007.07.046

[23] P. Liu, P. F. Borrell, M. Božič, V. Kokol, K. Oksman *et al.*, *J. Hazard. Mater.*, **294**, 177 (2015), https://doi.org/10.1016/j.jhazmat.2015.04.001

[24] C. H. Chan, C. H. Chia, S. Zakaria, M. S. Sajab and S. X. Chin, *RSC Adv.*, **5**, 18204 (2015), https://doi.org/10.1039/C4RA15754K

[25] N. Mohammed, N. Grishkewich, R. M. Berry and K. C. Tam, *Cellulose*, **22**, 3725 (2015), https://doi.org/10.1007/s10570-015-0747-3

[26] A. Pei, N. Butchosa, L. A. Berglund and Q. Zhou, *Soft Matter.*, **9**, 2047 (2013), https://doi.org/10.1039/c2sm27344f

[27] A. Pei, N. Butchosa, L. A. Berglund and Q. Zhou, *Soft Matter.*, **9**, 2047 (2013), https://doi.org/10.1039/c2sm27344f

[28] A. Isogai, T. Saito and H. Fukuzumi, *Nanoscale*, **3**, 71 (2011), https://doi.org/10.1039/C0NR00583E

[29] M. Hassan, L. Berglund, E. Hassan, R. Abou-Zeid and K. Oksman, *Cellulose*, **25**, 2939 (2018), https://doi.org/10.1007/s10570-018-1779-2

[30] A. El-Gendy, R. E. Abou-Zeid, A. Salama, M. A. Diab and M. El-Sakhawy, *Egypt. J. Chem.*, **60**, 1007 (2017), https://doi.org/10.21608/ejchem.2017.1835.1153

[31] R. E. Abou-Zeid, S. Dacrory, K. A. Ali and S. Kamel, *Int. J. Biol. Macromol.*, **119**, 207 (2018), https://doi.org/10.1016/j.ijbiomac.2018.07.127

[32] O. Nechyporchuk, F. Pignon and M. N. Belgacem, *J. Mater. Sci.*, **50**, 531 (2014), https://doi.org/10.1007/s10853-014-8609-1

[33] L. Segal, J. J. Creely, A. E. Martin and C. M. Conrad, *Text. Res. J.*, **29**, 786 (1959), https://doi.org/10.1177/004051755902901003

[34] A. S. Elfeky, S. S. Salem, A. S. Elzaref, M. E. Owda, H. A. Eladawy *et al.*, *Carbohyd. Polym.*, **230**, 115711 (2020), https://doi.org/10.1016/j.carbpol.2019.115711

[35] W. Chen, K. Abe, K. Uetani, H. Yu, Y. Liu *et al.*, *Cellulose*, **21**, 1517 (2014), https://doi.org/10.1007/s10570-014-0172-z

[36] S. Park, J. O. Baker, M. E. Himmel, P. A. Parilla and D. K. Johnson, *Biotechnol. Biofuel.*, **3**, 10 (2010), https://doi.org/10.1186/1754-6834-3-10

[37] A. Salama and P. Hesemann, *Int. J. Biol. Macromol.*, **111**, 762 (2018), https://doi.org/10.1016/j.ijbiomac.2018.01.049

[38] J. Ma, F. Yu, L. Zhou, L. Jin, M. Yang *et al.*, *ACS Appl. Mater. Interfaces*, **4**, 5749 (2012), https://doi.org/10.1021/am301053m

[39] R. Zhao, Y. Wang, X. Li, B. Sun and C. Wang, *ACS Appl. Mater. Interfaces*, **7**, 26649 (2015), https://doi.org/10.1021/acsami.5b08403

[40] L. Chen, Y. Li, S. Hu, J. Sun, Q. Du *et al.*, *J. Exp. Nanosci.*, **11**, 1156 (2016), https://doi.org/10.1080/17458080.2016.1198499

[41] X. Yang, H. Liu, F. Han, S. Jiang, L. Liu *et al.*, *Carbohyd. Polym.*, **175**, 464 (2017), https://doi.org/10.1016/j.carbpol.2017.08.007